

Parametric study of polycyclic aromatic hydrocarbon laser desorption

This article has been downloaded from IOPscience. Please scroll down to see the full text article.

2008 J. Phys.: Condens. Matter 20 025221

(<http://iopscience.iop.org/0953-8984/20/2/025221>)

View [the table of contents for this issue](#), or go to the [journal homepage](#) for more

Download details:

IP Address: 129.252.86.83

The article was downloaded on 29/05/2010 at 07:21

Please note that [terms and conditions apply](#).

Parametric study of polycyclic aromatic hydrocarbon laser desorption

C Mihesan¹, M Ziskind^{1,3}, E Therssen², P Desgroux² and C Focsa¹

¹ Laboratoire de Physique des Lasers, Atomes et Molécules (UMR 8523), Centre d'Etudes et de Recherches Lasers et Application (FR CNRS 2416), Université des Sciences et Technologies de Lille, 59655 Villeneuve d'Ascq Cedex, France

² Laboratoire de Physico-Chimie des Processus de Combustion et de l'Atmosphère (UMR 8522), Centre d'Etudes et de Recherches Lasers et Application (FR CNRS 2416), Université des Sciences et Technologies de Lille, 59655 Villeneuve d'Ascq Cedex, France

E-mail: ziskind@phlam.univ-lille1.fr

Received 22 July 2007, in final form 20 November 2007

Published 13 December 2007

Online at stacks.iop.org/JPhysCM/20/025221

Abstract

We present the use of a combined laser desorption/multi-photon ionization/time-of-flight mass spectrometry technique for the analysis of polycyclic aromatic hydrocarbon (PAH) solid samples. A thorough characterization of the first step (laser desorption) of this experimental technique has been performed. By varying the energy of the laser pulse, a specific response of each PAH has been evidenced for pure and mixed PAH sample desorption. This behaviour has also been studied with respect to the fragmentation processes. Similar studies on PAHs adsorbed on graphite evidenced the possibility of desorbing molecules from the adsorbed phase only, i.e. without a contribution from the graphite substrate. These findings represent important preliminary steps towards the final goal of setting up a completely characterized analytical method for the investigation of the adsorbed phase of soot particles generated in combustion processes.

(Some figures in this article are in colour only in the electronic version)

1. Introduction

Polycyclic aromatic hydrocarbons (PAHs) constitute a large class of compounds containing two or more aromatic rings. Present from the early stages of the combustion processes, they play an important role in soot inception, following a complex and partially unsolved mechanism of condensation, coagulation, aggregation and dehydrogenation [1]. Furthermore, the gaseous PAHs are adsorbed onto the soot matrix so formed. Physical and chemical properties of soot are intimately linked to the fuel employed and to the type of combustion process since these parameters affect the structure and the adsorbed phase (especially PAHs) of the soot particles. The fate of these particles in organism is not yet accurately established; however there is currently no doubt as to their carcinogenic potential. For example, Denissenko *et al* [2] have pointed out the role of benzopyrene-type molecules in lung cancer. A thorough

characterization of the adsorbed phase in various combustion conditions is therefore needed in order to address the chemical reactivity of the soot particles, with direct impact on the human health [3, 4].

While data on gaseous PAHs present in the combustion gas is abundant, the available information on adsorbed PAHs is still relatively limited [5–12]. We are developing an experimental set-up dedicated to such a characterization, with special focus on the dependence of the adsorbed phase on the combustion stage or the fuel nature. In order to provide a better understanding of the complex processes involved in the laser desorption/multi-photon ionization/time-of-flight mass spectrometry method we use [13–15], a three-step program has been adopted: (1) complete characterization of the laser desorption process on pure or mixed PAH samples; (2) use of 'surrogate' soot samples by adsorbing PAHs on carbon substrates (graphite, activated charcoal surfaces, black carbon or washed soot); (3) analysis of combustion soot samples. This paper presents preliminary results of the first two steps of the project. The influence of the laser pulse

³ Address for correspondence: UFR de Physique-Laboratoire PhLAM, Université de Lille 1, Bâtiment P5, bur. 037-59655 Villeneuve d'Ascq Cedex, France.

energy on the desorption yield of six different PAHs has been investigated. The results show a specific response for each PAH, defined by a desorption threshold, an optimum laser energy (maximum yield) and a working range. The selectivity of the method with respect to PAH fragments is also discussed. Similar studies on PAHs adsorbed on graphite are presented, evidencing the possibility to achieve a smooth desorption, i.e. without contribution of the carbon matrix to the mass spectrum recorded. Finally, some analytical implications are discussed.

2. Experimental technique

The main features of the laser desorption mass spectrometer have been presented in detail elsewhere [13–15]. Briefly, a 10 ns frequency—doubled (532 nm) Nd:YAG laser is focused ($\Phi \sim 1$ mm) at normal incidence on a PAH sample placed on a liquid nitrogen cooled sample holder in a UHV chamber (residual pressure $\sim 10^{-9}$ Torr). Cooling the PAH solid samples is necessary because of the high vapour pressure of these compounds at ambient temperature [16].

In contrast to our previous work [14] using an IR OPO to desorb PAHs by vibrational coupling of the energy, this paper presents the use of visible radiation (532 nm). The energy coupling into the solid is now performed through two-photon absorption, as all the PAHs under study have significant absorbance at 266 nm through the π - π^* transition of the aromatic ring [17].

The desorbed neutral particles expand into the region between the extraction plates of a 1 m long reflectron time-of-flight mass spectrometer (RM Jordan, Inc.) where they are photo-ionized by a 10 ns pulsed laser (Continuum Powerlite 8010, $\lambda = 266$ nm, 4.7 eV). Considering the ionization potential of the PAHs (typically 7–8 eV), two 266 nm photons are required to reach the ionization limit from the ground state. Two different geometries of the ionization laser beam are currently used by our group. The first one provides a larger ionization volume through the use of a cylindrical lens (to create a laser sheet of typical dimensions ~ 10 mm \times 10 mm \times 1 mm). This configuration greatly reduces the fragmentation related to the ionization step and can result in enhanced sensitivity [18]. The second geometry uses a spherical lens ($f = 25$ cm) for tighter focusing ($\Phi \sim 100$ μ m) of the ionization beam in the very centre of the desorption plume. This drastically increases the probability to fragment the desorbed molecules and, consequently to make the obtained spectra more complex. However, this geometry also greatly facilitates the ionization of fragments produced during the desorption step—particularly hydrogen and carbon (ionization potential 13.6 and 11.3 eV respectively, three-photon process). Thus, this geometry provides a more appropriate tool for the study of the desorption processes (including fragmentation) and we have chosen it for exclusive use in the present work. A typical ionization laser energy of ~ 30 mJ/pulse (leading to an intensity of ~ 40 GW cm $^{-2}$ at the focus point) has been used in the experiments described herein.

The desorption and ionization lasers are synchronized by a digital four channel delay/pulse generator (Stanford Research

System DG 535). The delay between the two lasers is set to 50 μ s. The transient signals delivered by the MCP mass spectrometer detector are recorded by a 2 GHz digital oscilloscope (LeCroy Waverunner 6200A) and then transferred to a PC through an Ethernet interface for further processing under Labview (National Instruments) environment.

The samples have been prepared by pressing ~ 300 mg of powder of six different PAHs: naphthalene (molecular weight 128 amu), acenaphthene (154 amu), phenanthrene (178 amu), anthracene (178 amu), pyrene (202 amu), and fluoranthene (202 amu). All of them are classified by the US EPA as priority pollutants [19].

3. Results and discussion

3.1. Specific response to the desorption laser energy

In order to give a better insight into the laser desorption process, we performed a study by varying the 532 nm laser pulse energy E_d . Figure 1 displays the evolution of the peak intensity of each PAH with E_d . We have experimentally checked that the use of the peak intensity or area led to qualitatively similar results. Please note that all the curves have been normalized; therefore, one should not use a direct comparison between the intensities of different PAH signals to evaluate the efficiency of the desorption/ionization processes for the various molecules under study.

This parametric study evidences a characteristic response of each PAH, defined by a desorption threshold, an optimum laser pulse energy for maximum yield and a working range. This can have important analytical implications in the analysis of complex samples or in the separation of isomers (see section 3.4 for a more detailed discussion). Furthermore, the studies we have performed on PAH mixture samples show that the specific response of each PAH to the desorption laser energy is preserved. Figures 2 and 3 illustrate this assertion in the case of 50–50 wt% pyrene/anthracene and acenaphthene/anthracene mixtures, respectively. The mass spectra included in these figures show the change in the observed PAH ratios when changing the desorption laser energy. Note that the pyrene has significantly higher ionization efficiency than anthracene at 266 nm [20], while acenaphthene and anthracene have comparable ionization cross sections at this wavelength. This could explain the much more spectacular change in the pyrene/anthracene ratio, compared to the acenaphthene/anthracene one. Although only a slight variation in the latter ratio is observed at high desorption energies (as expected from the responses of pure samples presented in figures 1(b) and (d)), this variation can still have important analytical implications when a quantitative approach is considered (see section 3.4). Note that in figure 2 the intensity scales on the two mass spectra are different and the signals have been normalized on the response profiles for better visibility. The important change in the ratio of the two compounds strengthens the need for a selective optimization of the experiment parameters (in this case, the desorption laser energy) in the (even qualitative) analysis of complex mixtures.

Another issue when looking to figures 2 and 3 is the mass resolution: as one can easily remark (especially from figure 3),

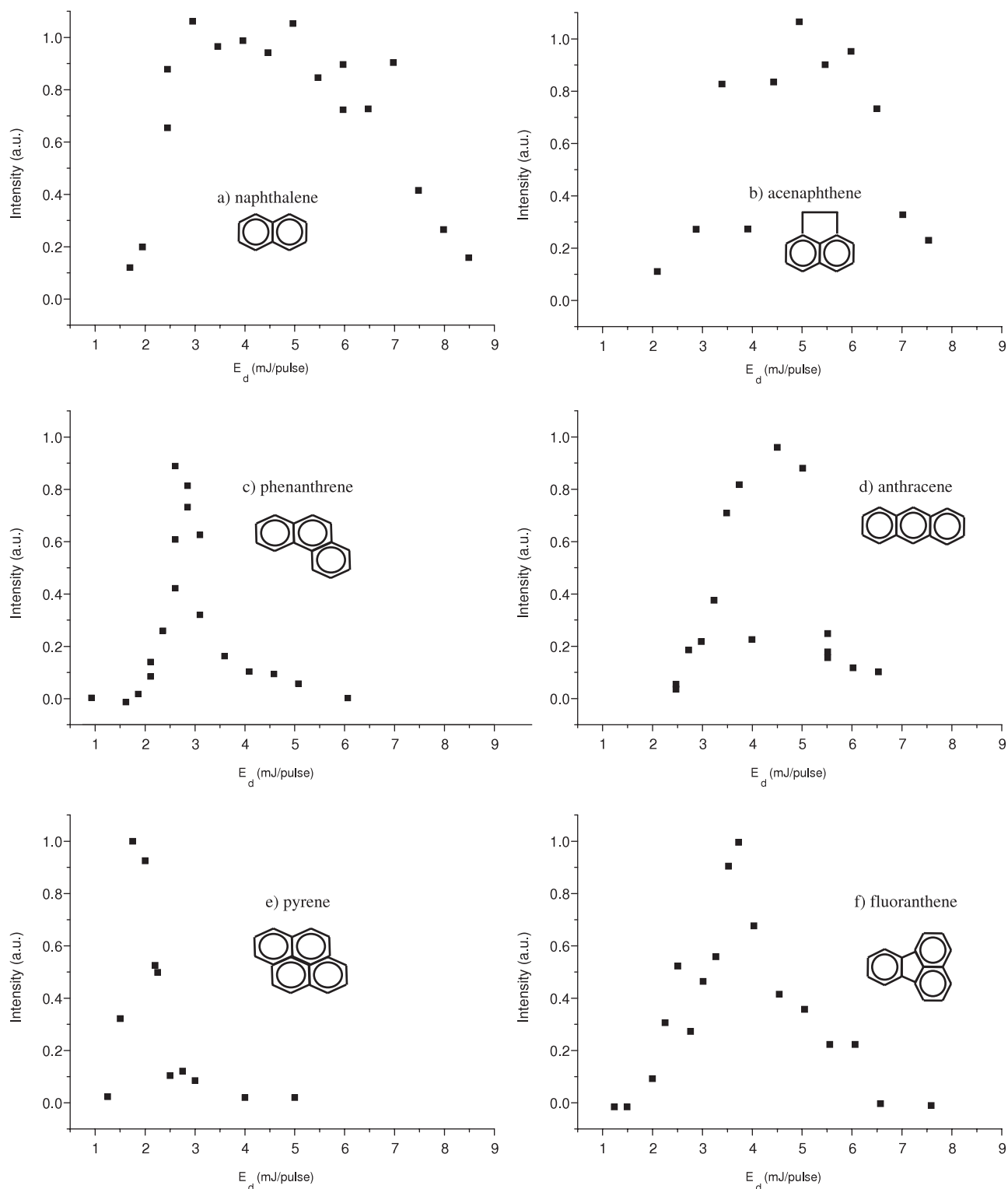


Figure 1. Response of the six PAH peak intensities to the desorption laser energy E_d .

this is heavily degraded at high desorption energies. As already mentioned in a previous study [18], this is not due to a mass spectrometer fault, but to a coupling of the ionization volume and ejecta internal energy effects. This behaviour will be addressed in a forthcoming study on the desorption/ionization coupling.

3.2. Role of the desorption in the fragmentation processes

The general evolution of the PAH signal intensities with E_d can be intuitively explained as follows: beyond a specific threshold, the energy brought by the laser to the sample is sufficient to eject the PAH; above this limit, the number of desorbed particles increases with E_d . However, the 'excess

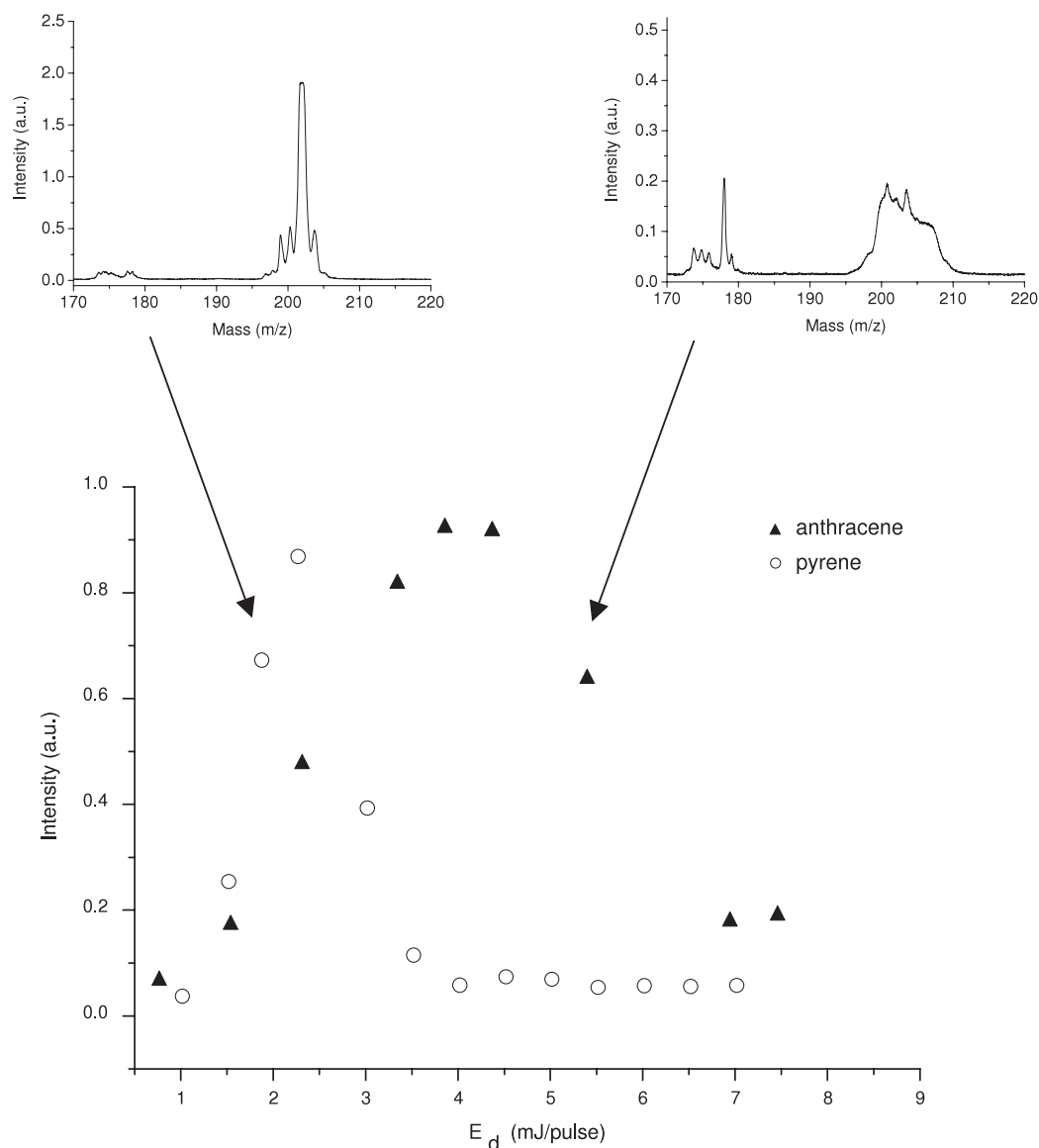


Figure 2. Evolution of the $m/z = 202$ and 178 amu PAH signals with E_d for the laser desorption of a 50–50 wt% pyrene/anthracene mixture. Above: mass spectra recorded at two individual energies (2 and 5.5 mJ/pulse).

energy' (with respect to the threshold) can also be used to fragment the molecules (i.e. directly at the desorption stage) or to increase the internal energy of the ejected particles, which further rises the fragmentation probability at the ionization stage. In addition, the multiplication of the collisions between the desorbed particles could also be responsible for the fragmentation. The competition between ejection and fragmentation explains the existence of an optimum laser pulse energy (maximum PAH signal intensity). Beyond this optimum, the fragmentation becomes predominant, the parent PAH signal intensity decreases while the signals of the lighter fragments become more intense. For higher desorption energies (between 2 and 6 mJ/pulse, depending on the PAH), the hydrocarbon radicals and larger fragments are further partially dissociated into carbon and hydrogen atoms. As an illustration, figure 4 displays the simultaneous evolution with E_d of the signals of phenanthrene (178 amu) and atomic carbon

(12 amu) for the desorption of a pure phenanthrene sample. One can notice that between the desorption threshold and the optimum of the PAH signal the carbon signal does not increase in the same way than that of the intact PAH. This emphasizes the role of the desorption process besides ionization in the formation of the lightest fragments even at low desorption fluences. Indeed, if one supposes the contrary, increasing the number of desorbed PAH molecules should result in the increase by the same factor of the fragments intensity, situation which is not observed here.

PAH peaks in the mass spectra are usually accompanied by polycyclic fragment signals in a wide range of E_d . The mass associated with these signals generally matches the mass of a PAH molecule or its (de)protonated and/or isotopic forms. Figure 5(a) shows the occurrence in the mass spectra of two high mass fragments at $m/z = 152$ and 176 amu when desorbing a pure fluoranthene sample ($m/z = 202$ amu). The

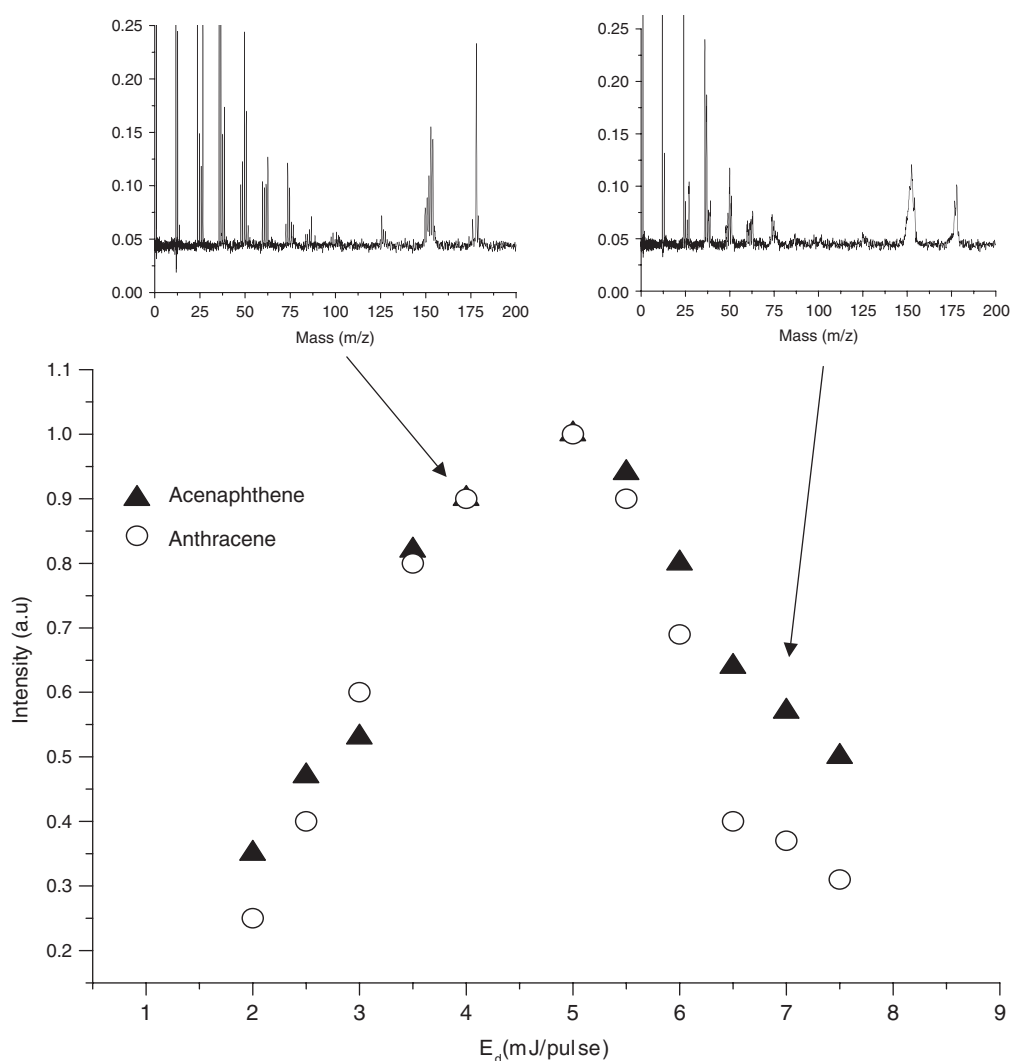


Figure 3. Evolution of the $m/z = 154$ and 178 amu PAH signals with E_d for the laser desorption of a 50–50 wt% acenaphthene/anthracene mixture. Above: mass spectra recorded at two individual energies (4 and 7 mJ/pulse).

mass 176 comes from the mass 202 (fluoranthene) by loss of a C_2H_2 ($m/z = 26$ amu) fragment, while the mass 152 comes from a subsequent loss of a C_2 ($m/z = 24$ amu) fragment. These fragmentation pathways have already been seen by other authors [21] and could drastically complicate the interpretation of the spectra, especially when analysing mixtures of several PAHs adsorbed on the same matrix. For instance, the m/z 152 would match the acenaphthylene PAH ($C_{12}H_8$), while the m/z 176 would match a dehydrogenated form of m/z 178 PAHs (anthracene, phenanthrene) obtained by loss of two hydrogen atoms.

Figure 5(b) shows the evolution with E_d of the 152 and 176 amu fragments intensity (for an easier comparison distribution for pure fluoranthene has also been replotted on figure 5(b)). Their behaviour resembles more to that of ^{12}C depicted on figure 4 or other light C_xH_y hydrocarbon radicals than to the behaviour of unfragmented desorbed PAHs. This confirms again the role of the desorption in the formation of all the fragments.

Moreover, from the analytical point of view, the specific response (in terms of desorption laser energy dependence) of

unfragmented molecules versus aromatic fragments matching PAH masses would allow one to say whether a given mass in the spectrum comes from an intact PAH (i.e. present in the analysed sample) or from the fragmentation of another (higher mass) PAH, also present in the sample.

3.3. Towards the analysis of soot samples: PAHs on graphite

As mentioned in section 1, the next step on the way to the analysis of soot samples (collected from a burner) is the study of PAHs adsorbed on graphite surfaces. Following the classification of Heimann *et al* [22], graphite is a regular allotropic form of carbon, containing hybrid sp^2 atoms only while soot is a transitional form, made of carbons with different hybridization states randomly arranged. As a result, graphite is a plane multi-layers structure, different graphene sheets being connected together by van der Waals forces. On the other hand, transmission electron microscopy studies have shown that soot exhibits an onion-like organization made out of small graphitic crystallites forming quasi-spherical carbon nanoparticles [23]. Despite this structural difference, soot

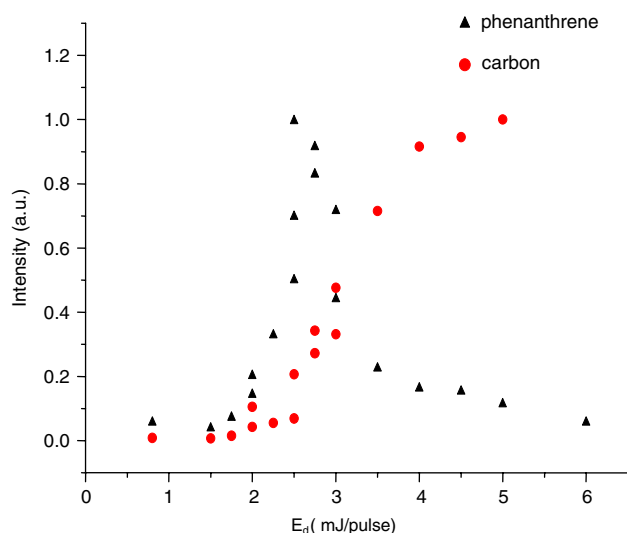


Figure 4. Evolution of the parent phenanthrene ($m/z = 178$) and ^{12}C fragment peak intensities with E_d .

particles can be roughly thought of as fragments of graphite growing due to successive additions of acetylene to a radical species followed by cyclization [24]. Thus, graphite can be reasonably used as model for the study of reactions on soot surface or of adsorbed PAHs onto atmospheric particles [25].

In our work, the main concern arises whether the ejected molecules during desorption of PAHs from graphite are representative of the adsorbed phase or are produced *in situ* on the substrate by pyrolytic processes due to laser irradiation [8, 26]. In order to give an insight on this issue, the response of a reference graphite sample, obtained by pressing 500 mg of pure powder (Sigma-Aldrich), to E_d has been studied (see figure 6). No signal all over the mass spectrum has been evidenced at low fluence until a carbon desorption threshold around 4.5 mJ/pulse is reached. Therefore, we conclude that in the E_d interval optimum for the PAHs detection, the carbon matrix does not contribute to signals

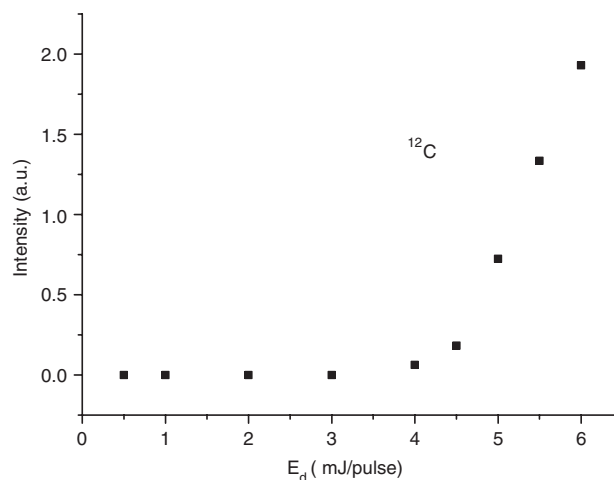


Figure 6. Evolution of the peak intensity of atomic carbon ($m = 12$ amu) desorbed from a pure graphite sample with E_d .

associated with PAH masses in the spectra. For energies above the desorption threshold, only C, C₂ and C₃ species have been observed. Supposing a similar structure for a soot particle, one can achieve (by judiciously choosing the laser pulse energy) a ‘smooth’ desorption process, i.e. to address only the adsorbed phase without desorption of the soot ‘skeleton’.

The next step consists in examining the behaviour of PAHs adsorbed onto graphite with regard to the desorption fluence. For this purpose, 1 g of pure graphite has been mixed with 5 ml of a 0.2 M fluoranthene solution in chloroform. The mixture is then filtered, washed in water and finally dried for 12 h at room temperature and pressure. The obtained powder is pressed and finally analysed following the procedure described above. Results are in good agreement with the previous observations (see figure 7(a)): at low fluence, fluoranthene is desorbed with an optimum efficiency around 3 mJ/pulse while signals corresponding to the carbon significantly rise around 4.5 mJ/pulse. Below this value, PAH signal disappears after about ten laser shots. The graphite surface has been

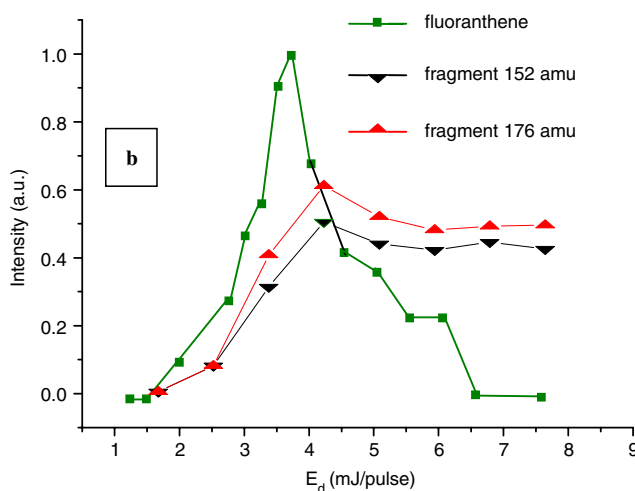
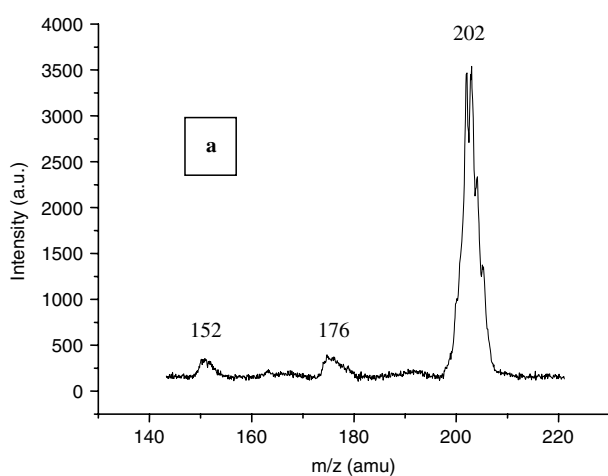


Figure 5. Laser desorption of a pure fluoranthene sample: (a) occurrence of two PAH fragments at 152 and 176 amu in the mass spectrum; (b) evolution with E_d of the two fragments and of the unfragmented molecule peak intensities.

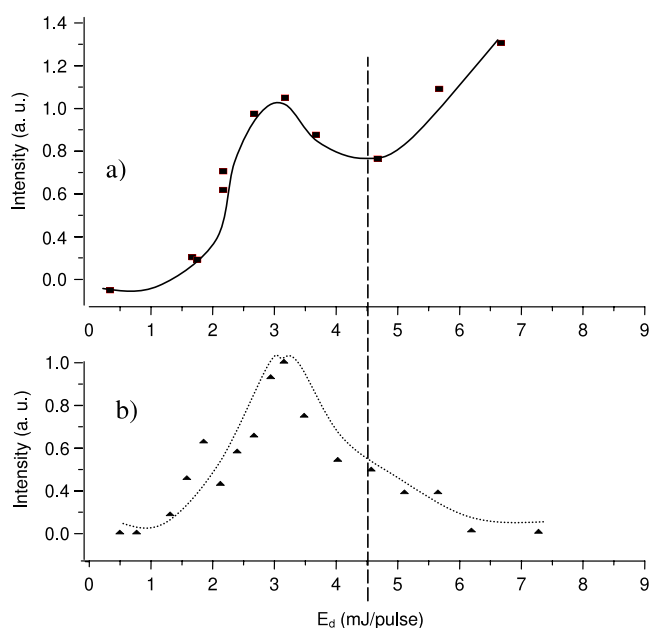


Figure 7. Evolution with E_d of the fluoranthene ($m/z = 202$ amu) signal for desorption of (a) fluoranthene adsorbed on graphite and (b) pure fluoranthene. The dashed vertical line corresponds to the graphite desorption threshold.

cleaned and the irradiation point has to be changed. Above 4.5 mJ/pulse, the PAH signal increases again and does not disappear after several thousand shots: the destruction of the carbon matrix presumably releases PAHs present in deeper graphene layers. Moreover, the desorption of fluoranthene is achieved in the same E_d interval as for a pure fluoranthene sample, as one can see from figures 7(a) and (b) (for an easier comparison, the E_d distribution for pure fluoranthene samples from figure 1(f) has been replotted on figure 7(b)). This last result is very promising in our effort to develop a completely mastered analytical method for the detection of PAHs adsorbed on combustion soot particles, i.e. we can reasonably tune the results obtained on pure PAH samples to PAHs adsorbed on carbon surfaces. A parametric study on PAHs adsorbed on other carbon surfaces like charcoal, black carbon or washed soot is underway in our laboratory in order to completely ascertain this hypothesis. Note that these substrates have structure, porosity and specific surface closer to those of soot when compared to graphite. First tests carried out on black carbon are very encouraging: the desorption threshold is comparable (slightly higher) to that for graphite, thus ensuring again a smooth desorption of PAHs in the low fluence range.

3.4. Analytical implications

The laser mass spectrometry (in various configurations, two-step or one-step desorption/ionization, time-of-flight or Fourier transform mass spectrometers) has been extensively used in the study of PAHs present in natural samples (or laboratory surrogates), like meteorites [26, 27], interplanetary dust particles [28], ancient terrestrial rocks [29], sediments and soils [30–34], combustion soot and particulate matter [5–12, 35–38], wood ash [39], aerosols [40, 41], or wa-

ter [42–44]. Although most of the studies in this (non-exhaustive) list looked at qualitative aspects, some of them tackled also quantitative issues. A critical examination of this approach by Zare and co-workers [45] revealed that changing various parameters of the analytical method (energy and wavelength of the desorption and ionization lasers, desorption/ionization delay, beam geometry) can induce important changes in the measured PAH ratios (in some cases up to a factor of 24). This behaviour is evidenced also in the present study, with respect to the desorption laser energy dependence (see e.g. the mass spectra in figure 3). This strengthens the idea that one cannot safely use a single functioning point to have a complete view of the sample under analysis, but should rather proceed by a prior ‘quality control’ study on the influence of different experimental conditions in the final result.

In a combined laser mass spectrometry/gas chromatography study on the presence of PAHs on geosorbents, the differences in the ionization efficiencies have been suggested to cause the observed discrepancy between the results obtained by the two methods [30]. In the light of the present results, we can speculate on a possible influence of the specific desorption behaviour of different PAHs. Another example is given by the analysis of a PAH mixture in soil samples [33] which exhibited an apparent series of desorption thresholds (plateaus followed by sharp rises) in the total ion signal evolution with the laser pulse energy (see figure 3 of [33]). The authors noticed important modifications in the recorded mass spectra with the change in the desorption fluence. This behaviour can find an explanation in the present results, as the different regions in this evolution could represent the onset for the desorption of new PAHs or for the fragmentation of existing PAHs.

On the other hand, fragmentation is a major concern in this analytical context, as one wants to avoid interference of the many different trace compounds of an environmental sample due to the similar masses of molecular or fragment ions, which can lead to erroneous identification of lower weight species. This motivated a number of studies on the wavelength (resonant versus non-resonant), pulse energy and temporal width (ns versus fs), especially at the ionization level [21, 46]. Beyond the analytical issues, fragmentation could also be seen as a tool to discriminate isomers (i.e. in a way similar to MS^n spectrometry, by generating different fragments with increasing desorption/ionization fluence). However, the PAHs are one of a very small class of compounds for which MS^n approaches are rather poor at distinguishing between isomers, as they all have relatively similar fragmentation spectra [32]. In this case, the use of the specific response to the desorption laser energy can offer a possibility to overcome this drawback (at least for some PAHs).

The usual intensities employed in the analysis of PAHs in natural samples by two-step laser mass spectrometry are in the range of 10^6 – 10^7 W cm $^{-2}$, both for desorption and ionization lasers [26, 38–40, 42]. The values we used for desorption in the present study ($\sim 10^7$ W cm $^{-2}$) are sensibly the same (though a direct comparison is not completely meaningful, as most of the previous studies used a CO $_2$ laser for vibrational heating, while we use 532 nm for electronic excitation), but they are much higher for the ionization step ($\sim 10^{10}$ W cm $^{-2}$,

average on the entire beam profile). The general use of low ionization intensities is favoured by the resonant character of the PAH ionization at 266 nm, which is the wavelength most commonly employed [9, 26–32, 38, 40]. The choice we made on the use of high ionization intensity was motivated by the need of enough photon density to ensure the ionization of fragments (e.g. atomic carbon) involving non-resonant three-photon mechanisms. Note however that comparable (or even higher, 10^{13} – 10^{15} W cm⁻²) ionization intensities have already been reported in studies on the fragmentation dynamics of laser desorbed PAHs [21, 46]. Although the high ionization intensities used here (to address rather fundamental issues) are not directly translatable to applied studies for the observation of unfragmented species from natural samples, the trends evidenced at the desorption level can give useful tools for a more accurate interpretation of the analyses. These results are to be corroborated with previous ones obtained at lower ionization fluences (by use of a cylindrical lens) [18]. Moreover, the intricate coupling between desorption and ionization parameters through the internal energy of the ejecta will be addressed in a forthcoming study.

The possible applied openings for the empirical finding described above should invite a more quantitative theoretical investigation of this behaviour. The experimental observation allows us to discriminate between some different PAHs (or between intact PAHs and fragments), but no prediction is currently available as to the expected response shape of one particular PAH. In particular, no link has been established between the structure of PAHs (e.g. naphthalene and anthracene, linear chains of cycles) or their mass (e.g. phenanthrene and anthracene: 178 amu, pyrene and fluoranthene: 202 amu) and their specific response. A modelling of the desorption process could be very useful (though very complex), both for technological and analytical applications and for a better understanding of the role played by the various parameters coming into the picture (thermodynamic properties of each PAH, dipole moment, mass, stability, etc) in the intricate laser–matter interaction.

4. Conclusion

This study investigates the 532 nm laser desorption process of six PAHs (in pure or mixture samples) with respect to the laser pulse energy. A specific response of each PAH has been evidenced, highlighting the need for individual optimization of experimental parameters in the analysis of complex samples. This method allows us also to discriminate between intact desorbed PAHs and fragments formed during the desorption process. Moreover, studies on PAHs adsorbed on graphite proved the capability of the technique to generate PAH signal from the adsorbed phase only, without a contribution from the carbon substrate. These studies are currently being extended to other carbon substrates, such as activated charcoal, carbon black or washed soot, in order to achieve the most complete characterization of the analytical method in view of its application to ‘real’ soot samples.

Acknowledgments

The Centre d’Etudes et de Recherches Lasers et Applications is supported by the Ministère chargé de la Recherche, the Région Nord-Pas de Calais and the Fonds Européen de Développement Economique des Régions. This research was supported by the Institut de Recherche en Environnement Industriel.

References

- [1] Miller J A, Volponi J V and Pauwels J F 1996 *Combust. Flame* **105** 454
- [2] Denissenko M F, Pao A, Tang M S and Pfeiffer G P 1996 *Science* **274** 430
- [3] Rhead M M and Hardy S 2003 *Fuel* **82** 385
- [4] Cignoli F, De Iulius S and Zizak G 2001 *Fuel* **80** 945
- [5] Dobbins R A, Fletcher R A and Chang H C 1998 *Combust. Flame* **115** 285
- [6] Hankin S M and John P 1999 *Anal. Chem.* **71** 1100
- [7] Marr L C, Kirchstetter T W, Harley R A, Miguel A H, Hering S V and Hammond S K 1999 *Environ. Sci. Technol.* **33** 3091
- [8] Bouvier Y, Mihean C, Ziskind M, Therssen E, Focsa C, Pauwels J F and Desgroux P 2007 *Proc. Combust. Inst.* **31** 841
- [9] Zimmermann R, Van-Vaeck L, Davidovic M, Beckmann M and Adams F 2000 *Environ. Sci. Technol.* **34** 4780
- [10] Haefflinger O P, Bucheli T D and Zenobi R 2000 *Environ. Sci. Technol.* **34** 2178
- [11] Carré V, Vernex-Loset L, Krier G, Manuelli P and Muller J F 2004 *Anal. Chem.* **76** 3879
- [12] Öktem B, Tolocka M P, Zhao B, Wang H and Johnston M V 2005 *Combust. Flame* **142** 364
- [13] Mihean C, Lebrun N, Ziskind M, Chazallon B, Focsa C and Destombes J L 2004 *Surf. Sci.* **566–568** 650
- [14] Mihean C, Ziskind M, Therssen E, Desgroux P and Focsa C 2006 *Chem. Phys. Lett.* **423** 407
- [15] Focsa C, Mihean C, Ziskind M, Chazallon B, Therssen E, Desgroux P and Destombes J L 2006 *J. Phys.: Condens. Matter* **18** S1357
- [16] Nass K, Lenoir D and Kettrup A 1995 *Angew. Chem. Int. Edn Engl.* **34** 1735
- [17] Karcher W, Fordham R J, Dubois J J, Glaude P G J M and Lighthart J A M (ed) 1983 *Spectral Atlas of Polycyclic Aromatic Compounds* (Dordrecht: Reidel–Kluwer)
- [18] Thomson K, Ziskind M, Mihean C, Therssen E, Desgroux P and Focsa C 2007 *Appl. Surf. Sci.* **253** 6435
- [19] *Evaluation and Estimation of Potential Carcinogenic Risks of Polynuclear Aromatic Hydrocarbons* 1985 (Washington, DC: Carcinogen Assessment Group, Office of Health and Environmental Assessment, Office of Research and Development, US Environmental Agency)
- [20] Haefflinger O P and Zenobi R 1998 *Anal. Chem.* **70** 2660
- [21] Robson L, Tasker A D, Ledingham K W D, McKenna P, McCanny T, Kosmidis C, Jaroszynski D A and Jones D R 2002 *Int. J. Mass Spectrom.* **220** 69
- [22] Heimann R B, Evsvukov S E and Koga Y 1997 *Carbon* **35** 1654
- [23] Popovicheva O B, Persiantseva N M, Kuznetsov B V, Rakhmanova T A, Shonija N K, Suzanne J and Ferry D 2003 *J. Phys. Chem. A* **107** 10046
- [24] Florio G M, Werblowsky T L, Müller T, Berne B J and Flynn G W 2005 *J. Phys. Chem. B* **109** 4520
- [25] Esteve W, Budzinskia H and Villenave E 2004 *Atmos. Environ.* **38** 6063

- [26] Messenger S, Amari S, Gao X, Walker R M, Clemett S J, Chillier X D F, Zare R N and Lewis R S 1998 *Astrophys. J.* **502** 284
- [27] Clemett S J, Chillier X D F, Gillette S, Zare R N, Maurette M, Engrand C and Kurat G 1998 *Orig. Life Evol. Biosph.* **28** 425
- [28] Clemett S J, Maechling C R, Zare R N, Swan P D and Walker R M 1993 *Science* **262** 721
- [29] Mahajan T B, Plows F L, Gillette J S, Zare R N and Logan G A 2001 *J. Am. Soc. Mass Spectrom.* **12** 975
- [30] Gillette J S, Luthy R G, Clemett S J and Zare R N 1999 *Environ. Sci. Technol.* **33** 1185
- [31] Ghosh U, Gillette J S, Luthy R G and Zare R N 2000 *Environ. Sci. Technol.* **34** 1729
- [32] Specht A A and Blades M W 2003 *J. Am. Soc. Mass Spectrom.* **14** 562
- [33] Alexander M L, Hemberger P H, Cisneros M E and Nogar N S 1993 *Anal. Chem.* **65** 1609
- [34] Dale M J, Jones A C, Pollard S J T, Langridge-Smith P R R and Rowley A G 1993 *Environ. Sci. Technol.* **27** 1693
- [35] Zimmermann R, Ferge T, Gälli M and Karlsson R 2003 *Rapid Commun. Mass Spectrom.* **17** 851
- [36] Dobbins R A, Fletcher R A and Lu W 1995 *Combust. Flame* **100** 301
- [37] Apicella B, Carpentieri A, Alfè M, Barbella R, Tregrossi A, Pucci P and Ciajolo A 2007 *Proc. Combust. Inst.* **31** 547
- [38] Mathieu O, Frache G, Djebaili-Chaumeix N, Paillard C E, Krier G, Muller J F, Douce F and Manuelli P 2007 *Proc. Combust. Inst.* **31** 511
- [39] Bente M, Adam T, Ferge T, Gallavardin S, Sklorz M, Streibel T and Zimmermann R 2006 *Int. J. Mass Spectrom.* **258** 86
- [40] Morrical B D, Fergenson D P and Prather K A 1998 *J. Am. Soc. Mass Spectrom.* **9** 1068
- [41] Öktem B, Tolocka M P and Johnston M V 2004 *Anal. Chem.* **76** 253
- [42] Emmenegger C, Kalberer M, Morrical B and Zenobi R 2003 *Anal. Chem.* **75** 4508
- [43] Bucheli T D, Haefliger O P, Dietiker R Jr and Zenobi R 2000 *Anal. Chem.* **72** 3671
- [44] Weikhardt C, Tönnies K and Globig D 2002 *Anal. Chem.* **74** 4861
- [45] Elsilä J E, de Leon N P and Zare R N 2004 *Anal. Chem.* **76** 2430
- [46] Murakami M, Mizoguchi R, Shimada Y, Yatsuhashi T and Nakashima N 2005 *Chem. Phys. Lett.* **403** 238